

# Multiple imputation via chained equations for elastic well log imputation and prediction

Antony Hallam

(Institute for GeoEnergy Engineering, Heriot-Watt University, United Kingdom)

Debajoy Mukherjee

(Department of Chemical Engineering, Indian Institute of Technology (IIT) Kharagpur, West Bengal 721302, India)

Romain Chassagne

(Institute for GeoEnergy Engineering, Heriot-Watt University, United Kingdom)

Keywords: MICE, well log imputation, machine learning, elastic log prediction

---

**This manuscript has been submitted for publication in Computers and Geosciences. Please note that peer review for this manuscript is pending and that it has yet to be accepted for publication. Subsequent versions of this manuscript may have slightly different or reduced content to meet publication guidelines. If accepted, the final version of this manuscript will be available from the publisher and a DOI link will be provided. Please feel free to contact the corresponding author; we welcome feedback.**

---

# Multiple imputation via chained equations for elastic well log imputation and prediction<sup>\*</sup>

Antony Hallam<sup>a,\*</sup>, Debajoy Mukherjee<sup>b</sup>, Romain Chassagne<sup>a</sup>

<sup>a</sup>*Institute for GeoEnergy Engineering, Heriot-Watt University, United Kingdom*

<sup>b</sup>*Department of Chemical Engineering, Indian Institute of Technology (IIT) Kharagpur, West Bengal 721302, India*

---

## Abstract

Well logging is an essential component in the petroleum industry for developing a proper understanding of the subsurface geology and formation conditions. Unfortunately, the measurements are rarely complete and missing data intervals are common due to operational issues or malfunction of the logging device. Therefore the imputation of missing data from down-hole well logs is a common problem in subsurface workflows. Recently, many different approaches have been utilised but they are often manual or generalise poorly. Machine learning has reignited interest in this field with promises of a more generic and simpler approach. We explore whether the chaining of machine learning for mutli-log imputation improves results by overcoming disparities in the patterns of missing data. We will focus this work on the elastic logs of compressional (DT) and shear (DTS) sonic along with the bulk density (RHOB).

*Keywords:* MICE, well log imputation, machine learning, elastic log prediction

---

<sup>\*</sup>This manuscript has been submitted for publication in Computers and Geosciences. Please note that peer review for this manuscript is pending and that it has yet to be accepted for publication. Subsequent versions of this manuscript may have slightly different or reduced content to meet publication guidelines. If accepted, the final version of this manuscript will be available from the publisher. A DOI link will be provided. Please feel free to contact the corresponding author; we welcome feedback.

<sup>\*</sup>Corresponding author

*Email addresses:* arh5@hw.ac.uk (Antony Hallam), debajoymukherjee98.iitkgp@gmail.com (Debajoy Mukherjee), r.l.chassagne@hw.ac.uk (Romain Chassagne)

## 1. Introduction

Well logs are digital measurements acquired during the drilling of petroleum wells (Tittman, 1986). They are an important source of information for subsurface specialists who utilise the data to guide exploration and development activity. The logs are acquired by lowering or conveying a number of specialised tools along the well bore whereby measurements are recorded periodically, typically on a scale of approximately 10 cm. Measurements cover a range of physical properties related to both the rock and formation fluid surrounding the well bore and are typically complimentary with some lithology dependent relationships between them. Unfortunately for a variety of mechanical and commercial reasons which are explored further in section two, well log suites for any given well are rarely complete and strategies are required to overcome gaps in the data to facilitate further analysis and subsurface workflows.

For geophysical analyses (of interest), the elastic logs of compressional (DT) and shear (DTS) sonic along with the bulk density (RHOB) are of particular interest. Whilst related to each other through the framework and composition of the measured rock they offer distinct information important to linking seismic data with the earth. Our focus in this paper is the accurate imputation of these elastic well logs. In downstream geophysical workflows, continuous logs are important for seismic inversion, velocity modelling, pressure prediction and synthetic well ties. Gaps in the elastic logs can compromise and complicate the quality and conclusions of workflows used to inform such studies.

Imputation of elastic well logs has been approached using many methods. Typical techniques may include manual editing with hand-drawn values, donor log splicing, linear interpolation, local or lithology based mean-value fill, singular log-log regressions and empirical relationships (e.g. Gardner et al. (1974) for sonic and density and Greenberg and Castagna (1992) for compressional and shear sonic). In simple cases with single wells and logs many of these approaches are sufficient. There are however limitations, and often a degree of subjectivity and interpretation required as the methods break down when applied to larger

31 databases of wells, or when substantial gaps exist in the logs. Quantitative  
32 methods are required in such cases and empirical relations or numerical rock  
33 models are often employed but these are sensitive to inherent model assumptions  
34 that introduce bias error. To overcome these limitations, models can become  
35 increasingly complex and rigid as additional model constraints and variables are  
36 added to handle variations due to depth, lithology and fluid content.

37 The recent explosion in data science methods and availability of large amounts  
38 of well log data present an opportunity to use a more automated statistics based  
39 approach which simplifies the imputation process, improving both accuracy and  
40 turnaround. The application of machine learning methods to well log imputation  
41 or prediction and with geosciences in general is not new (Dramschi, 2020). For  
42 example, commercial applications of earlier machine learning algorithms (artificial  
43 neural networks (ANN) and radial basis functions) have been used to predict logs  
44 from seismic data and attributes (Hampson et al., 2001; Russell et al., 2003) have  
45 existed for nearly 20 years. More recently, Lopes and Jorge (2018) applied log  
46 imputation and prediction to a data set of 1026 north sea wells using a variety of  
47 methods including Bayesian Ridge Regression (BRR), Artificial Neural Networks  
48 (ANN) and decision trees. Efforts were made to generate training gaps in the  
49 data that mirrored the observed gaps in the data set. Decision tree ensembles  
50 (Random Forest and Gradient Boosted Trees) were found to outperform all  
51 other methods.

52 Random forest (RF) methods have proved popular in multiple well related  
53 use cases. Hegde and Gray (2017) applied RF to a drilling efficiency optimisation  
54 task using only surface measurements and demonstrated that offset wells could  
55 be used to improve the drilling rate over short intervals. Feng et al. (2021)  
56 applied RF to a DTS prediction tasks on the Volve data set using a quantile  
57 approach to estimate output uncertainty.

58 Neural network (NN) methods have also proved popular with researchers.  
59 Churikov and Grafeeva (2018) explore the prediction of the gamma-ray log  
60 using NN, comparisons were made with linear interpolation with favourable  
61 results for the NN over large gaps. There have also been attempts to apply

62 deep NN methods and composite methods to log prediction problems. Jian et al.  
63 (2020) uses an ensemble learning machine combining 5 common ML algorithms  
64 including DNN in a density log prediction task. Ensemble learning machines  
65 are designed to overcome limitations in the algorithms used by combining the  
66 results of each method. The DNN was outperformed by gradient boosted tree  
67 algorithms both for accuracy and performance (DNN required three orders of  
68 magnitude more training time). The authors concluded that insufficient training  
69 data was available to make DNN more competitive. Ghaihi (2020) experienced  
70 similar problems with a feed forward neural network where lithological zones  
71 which contained insufficient data either over or under predicted the truth.

72 Comparisons of different ML algorithms with empirical regression models  
73 for predicting shear sonic logs are made by Bukar et al. (2019). The authors  
74 concluded that Gaussian Process regression was superior to other methods and  
75 importantly, that it could account for variations in fluid saturation. The fluid  
76 content of a rock is an important aspect of well logging and fundamental to  
77 downstream subsurface analyses. Similar results were found by Brown et al.  
78 (2020), where the downstream petrophysical analysis workflow was bypassed by  
79 training gradient boosted tree algorithms to predict petrophysical logs directly  
80 such as water saturation and porosity. Training data in this case must include  
81 expertly curated petrophysical logs with special attention paid to preprocessing  
82 of the input logs.

83 The application of certain types of machine learning can also have additional  
84 benefits. Diaz and Zadrozny (2020) apply radial basis functions (similar to BRR)  
85 to impute gaps in the gamma-ray log. This Bayesian approach incorporates the  
86 posterior imputation uncertainty providing confidence measures on the output.  
87 This additional information was used in subsequent geostatistical modelling. The  
88 approach used by Feng et al. (2021) for quantile RF is similar, but provides a  
89 measure of the ensemble prediction variance.

90 Many of the discussed literature propose approaches to feature engineering,  
91 a process for data improvement or augmentation to improve results. Churikov  
92 and Grafeeva (2018) applied smoothing to the logs to reduce noise going into

93 their NN models. Ghaithi (2020) found that including additional non-tool logs  
94 such as depth improved the overall fit of the data while Hegde and Gray (2017)  
95 suggest that derivative (deterministic) logs created by domain experts improved  
96 results.

97     Scaling and standardisation of the data is also an important feature engineer-  
98 ing pre-processing step. Feng et al. (2021) and Churikov and Grafeeva (2018)  
99 transform logs with a logarithmic response (such as resistivity) to a more linear  
100 scale. Most authors also mention removing bias and scale differences between  
101 input logs. Finally, Feng et al. (2021) tests feature space redundancy reduction  
102 using measures of feature importance and principle component analysis.

103     In general, all of these examples have only considered machine learning  
104 approaches that train for a single target log. This approach honors the input  
105 data but we hypothesise that imputed log values can become more accurate  
106 when input features are also imputed. Most machine learning algorithms also  
107 require the input feature set to be complete. Due to the nature of missing values  
108 in well logs this would significantly limit the sections of the well where models  
109 can be trained and applied. By approaching imputation of all input features  
110 simultaneously a greater portion of the well can be imputed for more accurately.  
111 Such an approach would also enable a wider variety of prediction models to be  
112 adopted, not just those that can handle missing values in the input.

113     To explore this idea, this study applies the multiple imputation via chained  
114 equation (MICE) algorithm (van Buuren and Groothuis-Oudshoorn, 2011).  
115 MICE is an imputation algorithm that does not specify a prediction strategy, thus  
116 within the framework of MICE we test three common machine learning predictors  
117 (gradient boosted trees, bayesian ridge regression and k-nearest neighbours). Our  
118 study explores how multi-stage imputation might improve the prediction results  
119 in diverse data sets when compared with single stage or direct prediction.

120     The method/s will be tested first by standard ML evaluation techniques  
121 (accuracy scores of mean square error, absolute error, explained variance and  
122 Pearson’s  $R^2$  factor), using a blind multi-well test where known values will be  
123 predicted by the model trained on other wells.

124 The adoption of machine learning requires the introduction of new terminology  
125 unfamiliar to a typical well logging audience. Within this paper we refer to  
126 logs and features. Feature is a common term use to describe vector inputs to  
127 machine learning algorithms. For our purposes, features have the same dimension  
128 size as the input logs, however feature engineering of the logs may be used to  
129 scale, transform or modify the input to improve prediction accuracy or to suit  
130 prediction algorithm limitations. If features are used in place of the input logs,  
131 the feature engineering must be reversible for the log to be recovered after  
132 imputation. An imputer or imputation strategy refers specifically to a workflow  
133 or algorithm used to fill missing values. Algorithms or models termed predictors  
134 are a component part of any imputation workflow, either an empirical model  
135 or in the case of this study, machine learning. Imputation workflows typically  
136 require at least one or more prediction models for each log being imputed.

## 137 **2. Data Imputation and Prediction**

138 The fundamental aim of data imputation is to accurately predict values which  
139 are missing from a data variable or data set to provide complete input variables  
140 for further analysis. When performing imputation it is important to consider the  
141 style or character of a data sets missing values as this can impact the imputation  
142 strategy and prediction algorithms used. In the context of data missingness,  
143 character refers to the overall fraction of missing values, the distribution of  
144 the missing values between features, the continuity of the missing values and  
145 correlation of missing values between features. The more a data set matches  
146 these criteria, the more difficult accurate and robust imputation of the data set  
147 will be. The reasons for missing values are generally specific to the experiment  
148 being performed but are commonly due to experimental restrictions, mistakes or  
149 failures.

150 There are many approaches to estimating missing values which range from  
151 simple mean or median estimates, to regression models. More recently machine  
152 learning algorithms have been gaining in popularity in the geosciences (Dramsch,  
153 2020). The efficacy of any method depends upon the type of data being imputed,

154 the quality and distribution of the known values and the complexity of the  
155 imputation model. It is important to consider the data being imputed, the way  
156 in which the imputed data will be further studied and analysed and the data set  
157 as whole when selecting an imputation strategy.

158 If the imputation model relies upon a stochastic approach - as most machine  
159 learning does - the robustness of the predictions will rely upon the completeness  
160 of distribution sampled by the available data. Stochastic style imputation models  
161 can generally not be used to predict unknown or unseen measurements. The  
162 available measurements should also be relatively free of noise, excluding outliers  
163 and bad or improper data which will skew the input distribution.

164 The missingness character of well logs is generally related to processes by  
165 which logs in any given well are acquired. From a macro perspective logs may  
166 be partially or entirely absent from a well, and at smaller scales, gaps occur  
167 for operational reasons or due to log editing and quality control processes. The  
168 reasons for not recording data are varied but commonly include; commercial  
169 considerations (cost and time), logging tool availability, mechanical failures  
170 of the measurement tools and drilling equipment and geometric constraints  
171 within the well bore and along the tool string. Bad data often occurs in cased  
172 hole logging, or due to the breakdown of borehole conditions (which is usually  
173 lithology dependent) and tool failures. Importantly for imputation, much of this  
174 missing data is not random but blocky and regular. As examples; the shallow  
175 sections of well bores, particularly in the Oil and Gas sector are not readily  
176 logged by all tools, also, casing points which interrupt logging often occur in the  
177 same formations due to borehole engineering design restrictions and lithologically  
178 unstable formations may result in a higher data failure rate. The cumulative  
179 effect of these problems can cause missing data to be non-random.

180 Well logs must undergo a large number of manual corrections which merge,  
181 depth align and normalise separate tool logging runs within wells. Logs are also  
182 often normalised across large well databases to correct for differences due to  
183 tool models and calibrations. Without these quality control steps and manual  
184 edits for bad or inconsistent data, subsequent tasks including imputation and



185 prediction may become compromised.

186 Finally, there are aspects of well logs and geology that strongly affect the  
187 capability of regression techniques. The geology can change rapidly in the  
188 vertical direction with each geological zone having distinct logging properties  
189 and characteristics. Over larger distances these zones can also change laterally  
190 as chronostratigraphic layers with common names differ lithologically. Logging  
191 tools also measure at different scales and distances away from the well bore, and  
192 may not necessarily be measuring the same volume of the formation. Single  
193 lithologies can also vary with depth, leading to non-stationary data over the  
194 depth range of a well. Wells intersecting common geology at distinctly different  
195 depths can have significantly different log-to-log relationships that need to be  
196 accounted for by any prediction model.

197 Multiple model types are suitable to well log imputation. Due to the quantity  
198 of data, regression using empirical models or user derived relationships are  
199 common. These models are often restricted to single lithological zones or localised  
200 fields and cumbersome to calibrate and implement. They are also generally  
201 one-pass models, relying upon the coincident available data to calculate trends.  
202 We use this paper to explore the application of iterative multiple imputation to  
203 well logs where imputed values are subsequently used to improve the estimates  
204 of other missing data until a convergence tolerance or iteration limit is obtained.

### 205 *2.1. MICE*

206 Multivariate imputation of chained equations (MICE) (van Buuren, 2007;  
207 van Buuren and Groothuis-Oudshoorn, 2011) is a multi-feature, prediction model  
208 agnostic imputation strategy. MICE supposes that the output of prediction  
209 models used for imputation can be improved by chaining together a series of  
210 imputation models for all input features (well logs). With each iteration of  
211 the complete feature set, the accuracy of the imputed values improves as bias  
212 in the prediction models is reduced (Azur et al., 2011). The order in which  
213 imputation proceeds can be random or based upon the completeness of features  
214 (Raghunathan et al., 2001; Varoquaux et al., 2015). Iteration is ceased when

215 imputation predictions converge towards a stable solution.

216 The MICE imputation strategy offers advantages in data sets with large  
217 amounts of randomly missing data. Here, random implies that the missingness  
218 of a value is not correlated with the value itself. By imputing for all values the  
219 MICE algorithm should improve predictors that rely upon complete samples in  
220 the input data set for training and prediction. In this way, partially complete  
221 sample points may still contribute towards the imputation predictions. MICE  
222 also avoids complications arising from joint modelling techniques where multi-  
223 variate distributions must be specified. MICE does this by imputing for each  
224 variable individually.

225 Apart from the requirement that data should be Missing At Random (MAR),  
226 there are few other assumptions in the MICE algorithm (Algorithm 1). The  
227 freedom to choose a prediction method leaves the user to implement a method that  
228 suits the data domain or distribution. Indeed custom predictors of constraints  
229 may be introduced to improve results (Azur et al., 2011; Raghunathan et al.,  
230 2001). Generalised prediction models are generally preferred due to the lack  
231 of user interaction or parameterisation required. In this paper we explore the  
232 performance of three well known prediction models, Bayesian Ridge Regression  
233 (BRR), K-Nearest Neighbours (KNN) and Gradient Boosted Trees (GBT).

234 As an imputation workflow, MICE appears to be well suited to imputing  
235 well logs. Although missing values in wells often occur in blocks or commonly  
236 are entirely missing. If the data set is sufficiently large however, it may still  
237 meet the MAR requirement. In this study, our focus on machine learning and  
238 stochastic predictors limits the accuracy where logs cannot be characterised  
239 through relationships with other input logs or features.

240 Finally, most predictors cannot sample beyond the known inputs (e.g. ex-  
241 trapolation is not possible). The input data must contain information sufficient  
242 to cover the distribution of the missing values to be impacted.

---

**Algorithm 1:** MICE Algorithm

---

```
Input: Features to be imputed; Prediction Models
Output: Imputed Features
/* The imputation can be based upon the percentage of
   missing values or at random. */
select Imputation Order;
 $\Phi \leftarrow$  list;
/* initialise imputation chain */
for each feature in input do
  | fill missing values using a starting guess;
end
while change in predictions > tolerance do
  | /* The input can be sorted randomly each loop or from the
  |    least missing to most missing feature. */
  | sort input;
  | for each feature in input do
  |   | train predictor;
  |   | impute missing values in feature;
  |   | append trained predictor to  $\Phi$ ;
  |   | update input;
  | end
end
```

---

243 *2.2. Predictor 1: Bayesian Ridge Regression*

244 Bayesian Ridge Regression (BRR) can be described as a Bayesian extension  
245 of the popular Support Vector Machine (SVM) regression algorithm (Tipping,  
246 2001). Both methods approximate the output from the training data by solving  
247 for the coefficients of a weighted sum of basis functions. Constraints are applied  
248 to the solution which penalise the number of non zero basis functions preventing  
249 over-fitting of the noise which results in good generalisation properties. BRR  
250 differs from SVM by introducing Bayesian inference to explicitly model the noise  
251 within the data, which is assumed to have a Gaussian distribution. BRR tends  
252 to require fewer basis functions, produces probabilistic estimates of the solution  
253 and has fewer restrictions on the basis function kernel (Tipping, 2001).

254 The implementation used by this paper (Varoquaux et al., 2015) maximises  
255 the marginal likelihood of the hyperparameters controlling the smoothness of  
256 the output and the shape of the prior noise Gaussian distribution to fit the data.

257 Although a probabilistic solution is returned, the predicted value will be  
258 taken as the highest probability point of the output distribution.

### 259 *2.3. Predictor 2: K-Nearest Neighbours*

260 K-Nearest Neighbours (KNN) regression, is a technique that lazily models  
261 a function by considering a distance weighted average of a neighbourhood of  
262 known values (Dubey and Pudi, 2013; James et al., 2013; Poloczek et al., 2014).  
263 The regression solution is only an approximation to the true function but the  
264 method is well suited to multi-dimensional problems such as well logs. Unlike  
265 BRR, KNN methods are non-parametric, and the distribution of the output is  
266 not prescribed by a specific model or prior distribution. This can be helpful  
267 when input logs are discontinuous or classification based such as for geological  
268 zones.

269 Key considerations when using KNN regression are related to the inputs  
270 and hyper parameters of the algorithm. KNN regression benefits from data  
271 standardisation (zero mean unit standard deviation) of the input data because  
272 the distance metrics are strongly affected by the input magnitude. The best  
273 value for  $k$ , the number of nearest neighbours, is often found experimentally. A  
274 larger value of  $k$  will tend to suppress noise but could blur the boundary between  
275 values.

276 With a large number of input features, points become increasing equidistant  
277 and the discrimination power of KNN can begin to degrade. To overcome this,  
278 pre-processing through dimensionality reduction may be helpful, such as principle  
279 component analysis to remove or consolidate redundant features.

280 There are multiple techniques to efficiently generate the neighbourhood of  
281 points. The naive, brute force approach is often supplemented for tree based  
282 algorithms where a setup phase is used to calculate cumulative distance between  
283 points as a network for easier retrieval later (Varoquaux et al., 2015).

284 The implementation of KNN utilised by this study uses an equal weighting  
285 between input features and measures distance via the euclidean distance between  
286 points. The method is also unsupervised, with the number of neighbourhoods

287 determined by the algorithm.

#### 288 *2.4. Predictor 3: Gradient Boosted Trees*

289 Gradient Boosted Tree (GBT) algorithms are a recent and relatively successful  
290 evolution of the decision tree machine learning algorithm. In a decision tree,  
291 input data is spread from the starting root through branches to decision split  
292 points whereupon it is routed into two new branches based upon a single logical  
293 operator. The operator used at each split can vary but generally aims to maximise  
294 the information gain or prediction accuracy after the split. Decision trees can  
295 continue to grow until they have a single data-point in each leaf but typically  
296 are limited to a maximum number of splits or depth. A single decision tree is  
297 generally a poor predictor for any model and they are termed weak learners.

298 Gradient boosting first used in AdaBoost (Freund and Schapire, 1997) seeks  
299 to transform decision trees from weak learners to strong learners by retraining  
300 recurrently against an objective and regularisation function. Standard objective  
301 functions can be solved using gradient descent style methods following the  
302 derivative of the error until a minimum is reached. Decision trees have no such  
303 derivative and as a result additive training (boosting) is used. In boosting the  
304 predictive tree functions are added after each training round until optimisation  
305 is achieved ensuring each decision tree is optimal prior to being included in the  
306 algorithm.

307 A single decision tree alone, even a gradient boosted tree still performs  
308 relatively weakly as a predictive tool. Predictive accuracy is greatly enhanced by  
309 employing ensemble methods. Random forests are a well known ensemble method  
310 that leverage a variety of statistical tools to create multiple unique decision  
311 trees. The accumulative results of multiple trees generates a significantly more  
312 accurate predictive model. To introduce tree diversity during training random  
313 forest algorithms randomly sample subsets of the input data set using bootstrap  
314 aggregation (bagging via representivity and independence). Data subsets will  
315 randomly sample both the feature space (dropping features) and the sample  
316 space (dropping samples) to generate a broad range of unique decision trees

317 within the forest.

318 There are many benefits to GBT and decision tree methods. Decision trees  
319 often scale well with data input, are fast and have a simplicity that does away  
320 with much of the pre-processing needs. They also avoid implicit regression models  
321 and are non-parametric (distribution agnostic) relying only on a logical (greater  
322 than or less than) operator at each decision branch. Decision trees also have  
323 transparency and can be inspected easily compared with other machine learning  
324 approaches such a neural networks. Finally, decision trees allow for manual  
325 tuning of the bias and variance error trade-off through their hyperparamters.

326 GBT also benefit from being able to accept missing values as input. Decision  
327 trees achieve this by considering whether a value is missing or not as the logical  
328 split, solving the remainder of the problem as normal. For this reason we include  
329 testing of direct or single pass imputation with GBT (referred in the rest of the  
330 document as D-GBT) as well as in a MICE approach.

331 There are many popular implementations of GBT available, but we utilise  
332 LightGBM within this study (Ke et al., 2017).

### 333 **3. Test Data, Preprocessing and Conditioning**

334 This study utilises two distinct well log data sets. The two data sets were  
335 selected due to their open availability, their preconditioning, comprehensive  
336 labelling and curation by subject matter experts. The two data sets also cover  
337 distinct spatial scales representing an increasing level of geological diversity and  
338 subsequent imputation difficulty.

339 Exact information about the preconditioning applied to the two data sets is  
340 not available but examination of the logs suggests the following processes have  
341 been applied and conditions have been met.

- 342 1. Logs from multiple tools runs have been depth aligned and merged to  
343 generate a single log for each measurement type.
- 344 2. Logs have been depth aligned using key markers.

- 345 3. Significant noise due to borehole conditions, logging through casing and  
346 other errors have been edited from the data. For Volve, this was performed  
347 by the authors.
- 348 4. Common logs (e.g. gamma-ray) have been normalised to account for  
349 variations in tool models and calibration settings.
- 350 5. Litho-stratigraphic interpretations provided with the training data are  
351 accurate and complete.

352 Appropriate preconditioning of the data prior to imputation is an important  
353 step. Performance of the imputation model, will be heavily dependent upon the  
354 quality of the input data.

### 355 *3.1. Volve*

356 The Volve data set comprises 20 wells from a single oil field in the Norwegian  
357 North Sea. The data was released by Equinor in 2018 as part of a complete  
358 field data set. The drilling of the wells spans approximately 20 years with initial  
359 exploration and appraisal wells often having more complete log suites (Hallam  
360 et al., 2020). In offshore field well log data sets, wells drilled later often have  
361 reduced logging programs due to commercial considerations and Volve follows  
362 this trend. The production wells drilled from 2007 on-wards are less likely to  
363 contain full logging suites and in particular, elastic logs.

364 Prior to any machine learning the Volve logs were first inspected in a stan-  
365 dard petrophysics package. The logs were analysed to identify sections which  
366 were either interpolated, incorrectly recorded or of general poor quality. Data  
367 determined to be unsuitable for model training was removed. The log data was  
368 then exported in LAS format to be loaded into Python for further analysis. The  
369 Equinor data set provided both raw and processed logs (logs with merged runs,  
370 depth shift corrections and other petrophysical quality control) as well as petro-  
371 physical interpretations (e.g. formation water saturation, total porosity). Apart  
372 from the formation tops, petrophysical interpretation logs were not included in  
373 this study.

374 The deepest part of the logs cover the reservoir and surrounding geological  
375 formations. For the remainder of this study the logs recorded shallower than the  
376 top Ty Formation have been removed. The total number of samples available  
377 for learning is 172 167. Within the filtered data set, log coverage varies greatly;  
378 Gamma-ray (GR) has almost no missing values for the zones of interest whilst  
379 shear-sonic (DTS) has over 60% missing values (Figure 1(a)). The three key  
380 elastic logs, density, compressional sonic and shear sonic have coverage of 80%,  
381 60% and 35% respectively.

### 382 *3.2. Force 2020 Well Log Machine Learning Data set*

383 A second larger test data set containing more than 90 wells from offshore  
384 Norway has been used to test the generalisation of this imputation methodology  
385 beyond closely related geological areas. The data set was originally created for  
386 the Force 2020 Machine Predicted Lithology (F2020) (Bormann et al., 2020)  
387 competition. Imputation of the missing values was a key step towards the  
388 objective of geological facies prediction.

389 The F2020 data set is provided in a pre-created train and test split. The split  
390 has been created arbitrarily by the data provider separating complete wells from  
391 training data. So called blind well testing is common in subsurface geosciences  
392 and are considered to offer a more realistic measure of the predictive capacity of  
393 models. The 10 test wells are evenly distributed within the input data, but the  
394 percentage of missing values per input log can vary dramatically between the  
395 training and test sets (Table 1).

396 The total size of the F20 data set is 1,307,118 samples with approximately  
397 10.5% belonging to the test set. There are a greater number of logs (features)  
398 made available with the F2020 data set which has missing values in the training  
399 data set per feature ranging from 0 - 95 %. The elastic logs DTC, DTS and  
400 RHOB have missing values of 6.9, 85.1 and 13.8 % respectively. Note that DTC  
401 is a common alias for DT and we use it here to remain consistent with the source  
402 data.

403 Due to the spatial extent of the data set, some of the additional logs provided



404 have been included as imputation constraints, namely, the Cartesian coordinates  
 405 of the sample (X\_LOC, Y\_LOC) but drilling metrics and non-critical logs with  
 406 a large proportion of missing values have been excluded, specifically bit size  
 407 (BS), rate of penetration (ROPA), mud-weight, and spectral gamma ray (SGR).

Table 1: Data sets log description and missing summary for imputed logs.

Description	Type	Log Pneumonic		Missing (%)			
		VOLVE	F2020	Volve Train	Volve Test	F2020 Train	F2020 Test
Well ID	Cat		WELL			0	0
Measured Depth	Cont		DEPTH_MD			0	0
Well Head Easting	Cont		X_LOC			0	0
Well Head Northing	Cont		Y_LOC			0	0
Well Head Elevation	Cont	TVDSS	Z_LOC	0		0	0
Stratigraphic Formation	Cat	ZONE	FORMATION	0	0	0	0
Caliper	Cont		CALI			4	0.03
Average Rate of Penetration	Cont		ROPA			54.13	45.5
Spontaneous Potential	Poten-Cont		SP			24.14	53.35
Medium Resistivity	Cont	RM	RMED	37.13	7.3	1.34	0.22
Deep Resistivity	Cont	RD	RDEP	15	0.08	0.01	0
Density	Cont	RHOB	RHOB	0.6	17.4	8.2	0.55
Density Correction	Cont		DRHO			10.22	7.44
Gamma-Ray	Cont	GR	GR	0.01	0	0	0
Neutron Porosity	Cont	NPHI	NPHI	0.7	0.04	30.41	13.7
Photo Electric Factor	Cont	PEF	PEF	18.32	7.27	38.7	5.8
Compressional Sonic	Cont	DT	DTC	19.97	9.49	4.6	0.55
Shear Sonic	Cont	DTS	DTS	38.12	20.05	84.1	64.1

### 408 3.3. Log Editing, Scaling and Feature Engineering

409 Log editing, transformations and scaling are necessary data cleaning processes  
 410 for most imputation algorithms. Significant edits are as per the beginning of this  
 411 section but scaling of logs to suit prediction algorithms is required. A common  
 412 process is to scale each sample of an input log  $x_i$  to to a new feature  $x'$  by the  
 413 mean  $\mu_x$  and standard deviation  $\sigma_x$  of  $x$  (Sarkar et al., 2018) sometimes referred

414 to as centering and scaling.

$$x'_i = \frac{x_i - \mu_x}{\sigma_x} \quad (3.1)$$

415 This removes inherent bias due to differences in scale and ensures all features  
416 cover a common range. The scaling factors  $\mu_x$  and  $\sigma_x$  are stored so that, after  
417 imputation logs can be returned to their original scale.

418 Some logs require additional consideration prior to imputation. Resistivity  
419 logs naturally exhibit a logarithmic scale inherent to the measurements made  
420 by the logging tool. To improve the linear correlation and low end sensitivity  
421 between the resistivity and other logs, they have been transformed through  
422 a base 10 logarithm. For example the deep resistivity is transformed to the  
423 imputation feature  $RES_{D10}$  via the relationship  $RES_{D10} = \log_{10}(RES_{D10})$ .

424 Categorical logs such as the Well ID and Stratigraphic Formation were  
425 transformed to numeric values through an integer encoder. For algorithms such  
426 as KNN regression, the distance between integers may affect the results. Adjacent  
427 or similar formations should therefore be given similar integer values. This is  
428 less critical for tree ensemble approaches.

429 We do not test the development of other features, but depending upon the  
430 data set, it may be useful to include other engineered logs such as smoothed  
431 variants of the raw input and other complimentary data types such as seismic  
432 traces or additional stratigraphic control like biostratigraphy labels. Due to the  
433 way sediments are deposited chronologically they can also be considered as a form  
434 of time-series. The algorithms applied in this study do not consider adjacency or  
435 the sequence of the data and prediction algorithms which account for a samples  
436 neighbourhood may perform better. Window based features could also be used  
437 to introduce neighbourhood information such as those offered by Christ et al.  
438 (2018) however, we suggest caution when doing this. Depending upon the size  
439 and frequency of the missing value gaps, many windowed or multi-sample based  
440 features could be difficult to compute accurately. Therefore, if attempting to  
441 use multi-sample dependent engineered features, special care should be exercised

442 around missing values.

### 443 *3.4. Feature Selection*

444 Feature selection, the task of choosing which logs or features to include in  
445 the imputation is often a difficult task. In some cases, exhaustive testing can  
446 be carried out to determine the correlation between data or impact upon the  
447 prediction algorithm. We defer to domain knowledge of the measured logs, as  
448 well as the percentage of missing values. Very sparse logs are excluded, except  
449 for the shear-sonic which we wish to predict even if missing. We also exclude  
450 engineering or borehole specific logs (e.g. caliper) that are not directly correlated  
451 with geological measurements.

### 452 *3.5. Data Testing and Preparation*

453 Data sets were first split into training and test data sets based upon wells.  
454 The Volve blind test wells were F-4, F-12, F-1 & F-15D. The testing split for  
455 the Force 2020 data set was provided with the data.

456 For training evaluation a further reduction of the training set was applied for  
457 each target log (DT, DTS, RHOB). This reduction created a unique training  
458 set for evaluating the predictive capacities of models for DT, DTS and RHOB  
459 individually. This approach was taken because aggressive sub-setting of all target  
460 logs would have over-decimated the training data set. For testing, a further  
461 30% of non-nan values were used from each target log. The data was removed  
462 in a random fashion, this contradicts the usual scenario where data is missing  
463 blockwise in logs but better meets the assumptions of the imputation models.

464 The high coverage of RHOB available in the Volve data set limited our  
465 ability to test the capacity for imputation when RHOB is not acquired. Thus,  
466 to augment and extend the testing of the Volve data set we introduce a block of  
467 missing RHOB values to simulation situations where all three elastic logs are  
468 missing.

## 469 4. Results

470 In this study, the models and predicted values were evaluated twice. First via  
471 a training set, where 30% of values were reserved for validation, and subsequently  
472 by using a test set containing a selection of blind wells. Both tests are evaluated  
473 based upon metrics for accuracy and variance of the imputed values. Imputation  
474 models were then tested against varying degrees of input sparsity (retraining for  
475 each level of sparseness) ranging from 10 to 90 %. Sparsity to the original data  
476 set was introduced randomly to all input features.

477 Further analysis was then conducted on the preferred models using SHAP  
478 (Lundberg and Lee, 2017) to better understand feature importance and followed  
479 by a qualitative assessment of the predictive capacity.

### 480 4.1. *Volve Log Imputation*

481 Imputation of the logs has been performed with seven different prediction  
482 approaches (Table 2). Four of these use the MICE algorithm and impute features  
483 with ascending order of missingness (MICE-BRR, MICE-O-BRR, MICE-KNN,  
484 MICE-O-KNN and MICE-A-GBT) and one model uses a random imputation or-  
485 der each iteration (MICE-R-GBT). Changing the order of imputation is designed  
486 to test assertions by Murray (2018) that randomisation between iterations can  
487 improve sampling statistics and bias.

488 For a comparison against the MICE tests we also perform direct imputation  
489 using GBT (D-GBT model). This is not possible for BRR and KNN models  
490 because they cannot handle prediction when the input features are incomplete.  
491 Instead, we perform imputation using just a single pass of MICE (one imputation  
492 model per input feature, MICE-O-BRR and MICE-O-KNN). All applications of  
493 MICE utilise the mean feature value as the initial guess for missing values.

494 To evaluate the models, five metrics for accuracy and bias are calculated,  
495 these are the explained variance, maximum error, mean absolute error (MAE),  
496 mean squared error (MSE) and Pearson's  $R^2$  or correlation factor. Explained  
497 variance and  $R^2$  values range from 0 to 1 with larger values indicating greater

Table 2: Imputation Model Descriptions

Name	Imputation Order	Description
MICE-BRR	Ascending	BRR using full MICE.
MICE-O-BRR	Ascending	BRR using MICE imputation for one iteration.
MICE-KNN	Ascending	KNN using full MICE.
MICE-O-KNN	Ascending	KNN using MICE imputation for one iteration.
MICE-A-GBT	Ascending	GBT using full MICE.
MICE-R-GBT	Random	GBT using full MICE..
D-GBT	N/A	Direct imputation of missing values using a single GBT model, no MICE.

498 correlation between truth and predicted logs. Error metrics range from zero to  
 499 infinity with smaller values indicating better performance.

500 Initially we consider the results from the validation sub-set (Table 3). For  
 501 Volve, the explained variance and  $R^2$  values are approximately  $\geq 0.9$  except  
 502 for the BRR model which performed poorly relative to KNN and GBT models.  
 503 Error rates exhibited similar trends with KNN and GBT models performing  
 504 consistently well.

505 Compared to the baseline single imputation models (Once) BRR and KNN  
 506 showed only small improvements or similar performance. The exception was for  
 507 the RHOB log imputations where performance degraded. The D-GBT model  
 508 showed similar or slightly worse performance than MICE approaches.

509 Metrics calculated using the test data were significantly lower (Table 4). The  
 510 explained variance and  $R^2$  metrics dropped to between 0.6 and 0.8. Overall,  
 511 error metrics also degraded increasing by 200-300%.

512 In Figure 3 we explore the link between geological zones, which define packages  
 513 of rock with similar properties (denoted by color). The correlation of the input  
 514 and predicted logs for three distinct model types; MICE-R-GBT, MICE-KNN  
 515 and MICE-BRR are plotted. The MICE-R-GBT results tend to show the tightest

Table 3: Metric scores for imputed values using different imputation algorithms on the Volve validation set. Best values are highlighted in bold.

Model	Log	Explained Variance	Maximum Error	Mean Absolute Error	Mean Squared Error	$R^2$
MICE-BRR	DTS	0.78	5.67	0.26	0.24	0.78
MICE-O-BRR	DTS	0.78	5.72	0.26	0.24	0.78
MICE-KNN	DTS	0.9	6.37	<b>0.14</b>	0.1	0.9
MICE-O-KNN	DTS	0.89	6.18	0.15	0.12	0.89
MICE-A-GBT	DTS	0.91	4.94	0.16	0.1	0.91
D-GBT	DTS	0.91	5.52	0.16	0.1	0.91
MICE-R-GBT	DTS	<b>0.92</b>	<b>4.61</b>	0.15	<b>0.08</b>	<b>0.92</b>
MICE-BRR	DT	0.87	14.3	0.23	0.14	0.87
MICE-O-BRR	DT	0.86	11.27	0.25	0.14	0.86
MICE-KNN	DT	0.92	3.58	<b>0.15</b>	0.08	0.92
MICE-O-KNN	DT	0.90	3.92	0.17	0.10	0.90
MICE-A-GBT	DT	0.93	<b>3.15</b>	0.16	0.07	0.93
D-GBT	DT	0.93	3.48	0.16	0.07	0.93
MICE-R-GBT	DT	<b>0.94</b>	3.36	<b>0.15</b>	<b>0.06</b>	<b>0.94</b>
MICE-BRR	RHOB	0.63	19.59	0.43	0.37	0.62
MICE-O-BRR	RHOB	0.65	19.6	0.43	0.34	0.65
MICE-KNN	RHOB	0.89	19.91	<b>0.17</b>	0.11	0.89
MICE-O-KNN	RHOB	0.90	19.92	0.17	0.10	0.90
MICE-A-GBT	RHOB	0.91	19.24	0.18	0.09	0.91
D-GBT	RHOB	0.91	<b>19.23</b>	0.18	0.09	0.91
MICE-R-GBT	RHOB	<b>0.92</b>	19.48	<b>0.17</b>	<b>0.08</b>	<b>0.92</b>

Table 4: Metric scores for imputed values using different imputation algorithms on the Volve test set. Best values are highlighted in bold.

Model	Log	Explained Variance	Maximum Error	Mean Absolute Error	Mean Squared Error	$R^2$
MICE-BRR	DTS	0.51	<b>2.2</b>	0.27	0.12	0.49
MICE-O-BRR	DTS	0.5	<b>2.2</b>	0.27	0.12	0.49
MICE-KNN	DTS	0.4	2.76	0.30	0.16	0.31
MICE-O-KNN	DTS	0.51	2.62	0.26	0.13	0.44
MICE-A-GBT	DTS	0.6	2.35	0.28	0.13	0.43
<b>D-GBT</b>	DTS	<b>0.69</b>	2.33	<b>0.20</b>	<b>0.09</b>	<b>0.63</b>
MICE-R-GBT	DTS	0.65	2.32	<b>0.27</b>	0.13	0.47
MICE-BRR	DT	0.69	6.55	0.36	0.32	0.65
MICE-O-BRR	DT	0.72	5.54	0.35	0.28	0.7
MICE-KNN	DT	0.72	3.75	0.36	0.28	0.69
MICE-O-KNN	DT	0.66	3.69	0.40	0.34	0.63
MICE-A-GBT	DT	0.78	4.03	0.31	0.21	0.77
<b>D-GBT Direct</b>	DT	<b>0.81</b>	<b>2.95</b>	0.29	<b>0.17</b>	<b>0.81</b>
MICE-R-GBT	DT	0.80	4.37	0.31	0.2	0.78
MICE-BRR	RHOB	0.44	8.29	0.58	0.65	0.38
MICE-O-BRR	RHOB	0.53	6.14	0.57	0.56	0.46
MICE-KNN	RHOB	0.63	6.22	0.39	0.41	0.61
MICE-O-KNN	RHOB	0.64	6.64	0.39	0.41	0.6
MICE-A-GBT	RHOB	<b>0.67</b>	<b>5.36</b>	<b>0.35</b>	<b>0.36</b>	<b>0.65</b>
<b>D-GBT</b>	RHOB	<b>0.67</b>	5.6	0.36	0.38	0.63
MICE-R-GBT	RHOB	0.65	5.65	0.36	0.39	0.63

516 correlation around the 1-1 line (perfect prediction). This is particularly true  
517 for the high slowness values in DTS. The MICE-BRR and MICE-KNN models  
518 both appear to under-predict DTS slowness at high values as well as RHOB in  
519 specific zones.

520 Overall, the D-GBT approach was the best imputer on the test data set for  
521 the three logs.

#### 522 *4.2. Volve Qualitative Analysis*

523 Here we use a qualitative analysis to gauge the suitability of the imputed  
524 results. Metrics provide a quantitative view of the data match but the imputed  
525 and predicted values must be assessed for their believability by a geoscience  
526 professional.

527 The BRR model results (Figure 4) show some interesting trends. The DT  
528 log appears to be well matched even where there are a high number of missing  
529 feature samples (between 10,000 and 15,000). Where the values for DT are high  
530 however, BRR appears to greatly over predict the DT log. A limited number  
531 of DTS values for testing were available but where they exist the MICE-BRR  
532 model seems to consistently under predict the slowness. There may be some  
533 bias from the other wells used for training against these samples. The RHOB  
534 predictions appear overly smooth compared with the known values, and they  
535 become inaccurate where the PEF and DRHO logs are absent.

536 The MICE-KNN model (Figure 4) matches the low frequency trends in  
537 the data but appears more prone to noise overall than the other models. The  
538 MICE-KNN model also returned no extrema beyond the models known values  
539 due to it's averaging approach. Compared with MICE-BRR, the MICE-KNN  
540 model better honours the known RHOB values without over smoothing but still  
541 struggles to eliminate the bias where PEF and DRHO are missing.

542 Both of the MICE-X-GBT models perform well, overall the predictions appear  
543 superior to MICE-BRR and MICE-KNN. The presence of the RHOB bias when  
544 missing DRHO and PEF suggest an inherent limitation between the available  
545 input features and the output.



546 Although the D-GBT model performed well in the metrics test we can build  
547 an appreciation for the limits of the method when analysing the qualitative  
548 results. Where the deliberate absence of any elastic values has been introduced  
549 between samples 25,000 and 31,000 (Figure 4) the quality of the prediction  
550 begins to break down for both RHOB and especially for DTS. The MICE  
551 implementation of GBT tends to outperform D-GBT in these situations where  
552 directly imputing for DTS from non-elastic logs is more difficult. It appears that  
553 sequential imputation tends to improve the overall prediction result in these  
554 extreme cases of many missing values. DTS for example with D-GBT imputation  
555 has a mean squared error of 0.36 in this specific test zone vs 0.06 for MICE-GBT.  
556 The results for RHOB are less convincing, 0.25 and 0.23 but the direct method  
557 can rely upon logs better suited to predicting RHOB which are available.

558 A single round of sequential BRR and KNN regression (MICE-O-BRR, MICE-  
559 O-KNN) also outperformed direct imputation via D-GBT with values for DTS  
560 MSE of 0.06 and 0.05 respectively.

#### 561 *4.3. Volve Log imputation error with increasing sparsity of input*

562 A key challenge to accurate imputation of well logs is the sparsity of the  
563 input. Sufficient training data is required to develop, calibrate and test a model.  
564 In this section we test the capabilities of the imputation models as sparseness  
565 is gradually increased in a random fashion to the input features. This is at  
566 odds with the often correlated missingness that occurs in individual wells but the  
567 limited size of the Volve data set necessitates this approach. On larger data sets  
568 a more blockly randomness could possibly be pursued.

569 As sparsity increase there is an identifiable decrease in accuracy for all  
570 predictors. The change is more systematic when measuring the validation results  
571 as compared with the rest results (Figures 5). Also, the results for MICE  
572 imputers are very similar to the baseline once or direct approaches.

573 BRR continues to underperform reaching a critical point of failure at a  
574 sparsity fraction of 0.5. The failure point for the other models tested appears at  
575 a sparsity fraction closer to 0.7. There is some jitter once BRR has failed which

576 may be related to the distribution of missing values within zones.

577 The results when applying to the test data set were slightly different. At  
578 high sparsity the GBT-MICE model appears to outperform the D-GBT model.  
579 Breakdown of the models occurs around 50% sparsity.

#### 580 4.4. *Volve Feature importance analysis*

581 The recent increase in the application of machine learning has also seen the  
582 development of techniques and methods designed to better explain the influence  
583 of input features on model outcomes. When there are a large number of input  
584 features it can be difficult to interpret why models behave the way they do  
585 and tailored workflows are required to establish causal links between input  
586 and output. One approach is the specialist algorithmic interpreter based upon  
587 Shapley Additive Explanations (SHAP) (Lundberg et al., 2020). SHAP uses  
588 game theory to assigns an impact score to a feature based upon the model output.  
589 Repeated stochastic testing of the model results in an overall view of how inputs  
590 affect the model output.

591 SHAP is well suited to explaining decision tree type algorithms and we  
592 apply SHAP here to our MICE-A-GBT model to better understand results and  
593 limitations of the model. To investigate the stability and importance of features  
594 during MICE iteration (specifically for the elastic target logs), we compare the  
595 second imputation round SHAP values to the last imputation round SHAP values  
596 (Figure 6). SHAP value swarm charts are generally interpreted by looking at  
597 the distribution of SHAP value impact. Input features with high importance  
598 are located at the top of the chart, they will have a large number of values  
599 distant from the origin (SHAP impact of zero) and cover a large range. The  
600 colour of the values indicates the direction in which the output feature is moved  
601 relative to the input feature. Features with less importance will cluster around  
602 the origin and have a small overall range. The number of clusters appearing  
603 along any features SHAP profile may indicate multiple distributions within a  
604 model (emphasising the need for non-parametric predictors).

605 For the MICE-A-GBT models the top three features tend to remain stable

606 between the second and last imputation rounds. There is a reordering of the  
607 lesser features, but their impact values are often considerably smaller.

608 For the DT log, DTS, RHOB and NPHI are the top three logs in importance.  
609 The strong link between DT and DTS (the compressional and shear sonic  
610 slowness) is not surprising, but DTS is one of the least sampled logs in the Volve  
611 data set so its availability to inform DT is limited. RHOB and NPHI which are  
612 much more frequently sampled are likely contributing much of the information  
613 used to fill the DT missing values. Pseudo lithology logs like GR are evaluated  
614 by SHAP as having a very low impact upon the DT output.

615 DTS, one of the least sampled logs relies heavily on DT, this is the inverse  
616 relationship from previously. Most surprisingly, the ZONE (lithological forma-  
617 tion) and deep resistivity logs (LogRD) occupy second and third position in  
618 importance. The ZONE SHAP values also operate in an inverse direction to  
619 the output values. This suggests that low value ZONES (shallow lithology) are  
620 increasing the output DTS whilst high value ZONE (deep lithology) are reducing  
621 DTS. In this case, ZONE may be acting as a proxy for depth, where natural  
622 compaction and increasing geological age generally decreases slowness. DTS is  
623 also more sensitive to rock competency than DT which is a complex function of  
624 mineral composition and micro-rock structure. Whilst the ZONE log does not  
625 inherently contain information about these properties it does group samples into  
626 common blocks that may aid with DTS prediction.

627 The RHOB models have the broadest reliance upon input features of the  
628 three target logs. DT, PEF, GR and NPHI all appear consistently with high  
629 impact.

630 In all cases, the features with the highest impact have a common distribution  
631 of SHAP values across imputation rounds indicating stability in the import and  
632 influence of key features during MICE iterations.

#### 633 *4.5. Force 2020 Log Imputation*

634 For the FORCE 2020 data set we follow the same imputation procedure of  
635 train, validate and test that was applied to Volve data set. KNN type models

Table 5: Metric scores for imputed values using different imputation algorithms on the F20 validation set. Best values are highlighted in bold.

Model	Log	Explained Variance	Maximum Error	Mean Absolute Error	Mean Squared Error	$R^2$
MICE-BRR	DTS	0.83	5.74	0.3	0.17	0.83
MICE-O-BRR	DTS	0.83	5.77	0.3	0.17	0.83
MICE-A-GBT	DTS	0.94	4.8	0.16	0.06	0.94
MICE-R-GBT	DTS	0.93	<b>5.47</b>	0.16	0.07	0.93
D-GBT	DTS	<b>0.95</b>	5.55	<b>0.15</b>	<b>0.05</b>	<b>0.95</b>
MICE-BRR	DT	0.83	4.26	0.25	0.17	0.83
MICE-O-BRR	DT	0.83	4.3	0.25	0.17	0.83
MICE-A-GBT	DT	0.95	<b>3.16</b>	<b>0.11</b>	0.05	0.95
MICE-R-GBT	DT	0.94	4.02	<b>0.11</b>	0.06	<b>0.94</b>
D-GBT	DT	<b>0.96</b>	3.43	<b>0.11</b>	<b>0.04</b>	0.96
MICE-BRR	RHOB	0.7	10.2	0.39	0.3	0.7
MICE-O-BRR	RHOB	0.74	5.56	0.37	0.26	0.74
MICE-A-GBT	RHOB	<b>0.91</b>	5.38	<b>0.2</b>	<b>0.09</b>	0.91
MICE-R-GBT	RHOB	<b>0.91</b>	<b>5.33</b>	<b>0.2</b>	<b>0.09</b>	0.91
D-GBT	RHOB	<b>0.91</b>	5.33	<b>0.2</b>	<b>0.09</b>	<b>0.91</b>

636 were excluded from testing due to technical problems applying the method to  
637 the size of the data set.

638 All of the GBT type models again performed the best both in the training  
639 (Table 5) and testing (Table 6). The MICE-GBT models perform slightly better  
640 for DTS and much better for DT when compared with the D-GBT approach.

641 Qualitative analysis for the test results indicate a very good fit for the test  
642 data. In places, the BRR model is prone to generating large noise spikes in  
643 the DTS log (between samples 19,000 and 42,000, Figure 7). The noise spikes  
644 don't appear to be associated with any particular missing log and are perhaps  
645 due to a lack of training in a particular zone. Comparatively, the GBT logs  
646 show a consistently good fit outperforming the other models and validating  
647 the quantitative metric results. The fit to the long wavelength variations is  
648 particularly strong.

649 An analysis of the relationship between metric based prediction performance

Table 6: Metric scores for imputed values using different imputation algorithms on the F20 test set. Best values are highlighted in bold.

Model	Log	Explained Variance	Maximum Error	Mean Absolute Error	Mean Squared Error	$R^2$
MICE-BRR	DTS	0.89	2.44	0.22	0.09	0.89
MICE-O-BRR	DTS	0.89	2.4	0.23	0.09	0.89
MICE-A-GBT	DTS	0.92	2.59	0.18	0.07	0.92
MICE-R-GBT	DTS	<b>0.94</b>	2.54	<b>0.16</b>	<b>0.05</b>	<b>0.94</b>
D-GBT	DTS	0.93	<b>2.65</b>	0.18	0.06	0.93
MICE-BRR	DT	0.88	2.16	0.21	0.1	0.88
MICE-O-BRR	DT	0.87	2.25	0.2	0.1	0.87
MICE-A-GBT	DT	<b>0.94</b>	2.08	<b>0.16</b>	<b>0.05</b>	<b>0.94</b>
MICE-R-GBT	DT	0.91	<b>3.01</b>	0.17	0.07	0.91
D-GBT	DT	0.88	2.22	0.19	0.1	0.87
MICE-BRR	RHOB	0.72	4.82	0.37	0.26	0.72
MICE-O-BRR	RHOB	0.77	4.18	0.34	0.21	0.77
MICE-A-GBT	RHOB	0.86	4.01	0.25	0.13	0.86
MICE-R-GBT	RHOB	<b>0.87</b>	<b>3.83</b>	<b>0.24</b>	<b>0.12</b>	<b>0.87</b>
D-GBT	RHOB	<b>0.87</b>	4.0	<b>0.24</b>	<b>0.12</b>	<b>0.87</b>

650 and the number of samples available for training within each geological formation  
651 (Figure 8) show erratic trends in performance when the training sample size  
652 is small. As the number of samples in a geological zone increases beyond  
653 approximately 20,000 points both MAE and MSE metrics trend towards a more  
654 stable value. Trends in  $R^2$  and explained variance are less clear.

## 655 5. Discussion

### 656 5.1. Explanation of Results

657 On the whole, multiple iterations of the MICE algorithm do not appear to  
658 improve the overall predictive capacity of the models implemented. There are  
659 exceptions where certain combinations of missing logs and sequential imputation  
660 and prediction are desirable but this does not appear to form the bulk of missing  
661 values in the tested data sets. GBT generally out performed the BRR and KNN  
662 models. The ability for GBT to handle missing values is a significant advantage  
663 with performance as good or better than the MICE-GBT method.

664 The exceptions where MICE improves upon direct imputation were observed  
665 when the elastic logs were all missing. In these scenarios complete prediction of  
666 all three targets is required and accuracy improves when sequential imputation is  
667 performed. In these cases, the more complex non-parametric relationships between  
668 logs are handled better. For example, DRHO may be used to predict RHOB  
669 which is subsequently used to predict DT and then DTS.

670 Although MICE is relatively inexpensive for log data it is computationally  
671 more expensive than direct or single pass sequential imputation. MICE typically  
672 runs for 10-20 iterations requiring multiple imputation predictors to be trained  
673 and stored.

674 Of the three machine learning predictive models tested, GBT appears to be  
675 a clear leader, exhibiting superior correlation and lower error. The strength of  
676 the ensemble approach over BRR and KNN may reflect a superior capacity to  
677 identify and model the complex non-parametric relationships between logs.

678 An observation from both data sets was the relative under performance of  
679 models in geological zones with small sample sizes, which was to be expected. A

680 subsequent analysis calculating metric scores for each zone (Figure 8), identified  
681 significant variations in metric scores for the test logs when sample sizes are small.  
682 We attribute the variance in the scores at small sample size to complex and  
683 multi-factored interactions between the available training samples, the sparsity  
684 of the input features for the zone and the effectiveness of cross-training between  
685 lithologically similar zones. The zones with larger sample sizes tend to exhibit  
686 more stable metric behaviour leading us to suspect insufficient data both for  
687 training purposes, and for the data available to calculate representative metric  
688 scores at the zone scale.

689 At larger sample sizes, there is a compression in the error variance across zones  
690 (particularly for the error metrics MSE/MAE) which may provide indicators  
691 for the number of samples needed in a zone to achieve some stability in the  
692 prediction model.

693 A more robust approach over using geological zones may be to consider  
694 undertaking this analysis based upon lithological characteristics rather than  
695 formation names. This could be achieved either via manual labelling, grouping of  
696 similar zone labels or, if the sample set is sufficiently dense, automated clustering.

697 Empirical models for elastic logs rely upon and emphasise their strong corre-  
698 lations. The SHAP analysis of the GBT approach confirms the interdependence  
699 of the elastic input features for accurate prediction (even with non-parametric  
700 methods) but intrinsically extends them to include other features as further  
701 control upon the model output. For example, while typical empirical workflows  
702 for prediction of compressional sonic from density would require additional cor-  
703 rections for depth and fluid content, the GBT model can leverage other input  
704 features such as sample depth and the resistivity to form better predictions.  
705 This greatly simplifies the entire workflow, and we would recommend utilising  
706 GBT for imputation.

## 707 *5.2. MICE limitations and assumptions*

708 All imputation or prediction methodologies rely upon a sufficient quantity of  
709 data to correctly calibrate the model and MICE is no different. If characteristi-

710 cally unique sections of log are missing from the training data, the predictive  
711 models will be unable to reproduce such data with any accuracy. This limits the  
712 application of MICE to data sets with representative sampling but is a common  
713 problem to all parts of machine learning; the machine cannot model what it has  
714 not seen. This leads to poor generalisation of the model unless the training data  
715 set is sufficiently diverse. In practice, and for well log imputation, the pragmatic  
716 approach would be to tailor an imputation model for each unique input data set.  
717 The cost of training, at least with the models tested was acceptably low (on the  
718 order of minutes), but for more costly prediction models further consideration  
719 may be required.

720 There is also a degree of non-repeatability with most ML predictors and  
721 therefore any application of MICE will be limited by the chosen prediction  
722 algorithm. If the input data set is augmented or changed, the output predictions  
723 and imputations are also likely to change. The degree of difference observed  
724 will depend upon the degree of changes to the input and the dependence upon  
725 randomness in the training of the prediction models. The non-repeatable nature  
726 of the imputations may discourage downstream users of the data who require  
727 stable logs as input to their own workflows. In these cases the general prediction  
728 capability of ML regression models must be traded off against the labour intensive  
729 but more stable empirical or manual prediction approach. A possible solution  
730 could be to capture and store multiple imputed versions as a measure of the  
731 imputation uncertainty in a manner similar to but distinct from Diaz and  
732 Zadrozny (2020).

### 733 *5.3. Hyperparameter Tuning*

734 MICE has relatively few hyperparameters; maximum iterations, convergence  
735 tolerance and imputation order. For this study, imputation order, either random  
736 or ascending did not appear to greatly influence the results and maximum  
737 iterations and convergence tolerance were left at their default values.

738 MICE-GBT and the direct GBT were together the best prediction models  
739 tested in this study. Both were submitted to a four hyperparameter tuning grid



740 search that varied the minimum leaf size, the maximum tree depth and the  
741 bagging frequency and fraction.

742 In general it was found that the bagging parameters had little effect upon  
743 the overall results although very low bagging fractions ( $<0.2$ ) tended to cause  
744 training issues and should be avoided. There was no benefit to the prediction  
745 metrics when the maximum depth of the trees was set at greater than 7. Larger  
746 tree depths should probably be avoided to prevent over fitting. Increasing the  
747 minimum leaf size tended to decrease the maximum error, preventing out-liers  
748 in the prediction but at the expense of over generalising the solution and in turn  
749 increase the mean squared error. From the metrics, the optimum minimum leaf  
750 size was determined to be around 300 for the MICE implementation and 500 for  
751 the direct method.

752 Comparisons of the base and tuned model outputs demonstrated little to no  
753 improvement for the direct prediction models and some improvement when using  
754 tuned parameters within the MICE methods. Some instability in the result was  
755 observed when a minimum leaf size of 300 was used for the iterative method  
756 and reducing this to 200 greatly improved the results. The improvements in  
757 prediction accuracy for the MICE models were most notable in the RHOB log  
758 results where a bias in the result is removed.

#### 759 *5.4. Further research*

760 Although the authors would recommend the use of MICE or indeed direct  
761 imputation using the machine learning models tested, there are additional tests  
762 that may improve our application and understanding of MICE for well log  
763 prediction and imputation. For training validation, we use randomised selection  
764 of points within logs. This is not typically how gaps occur in well log data.  
765 Alternative approaches such as the method employed by Lopes and Jorge (2018)  
766 of pseudo modelling the gaps may further test the robustness of our approach.  
767 Validation tests could also be augmented to check for over-training by utilising  
768 k-fold cross-validation methods common in machine learning.

769 We also suggest that the MICE algorithm might be modified to improve

770 and or automate noise or bad data rejection. Currently, log editing is required  
771 beforehand to quality control the input, the MICE process may be a tool that  
772 can identify and automatically remove data which fails a tolerance criterion when  
773 compared with predictions. Initial imputation values use by MICE methods  
774 could also be improved by using empirical relationships rather than the mean  
775 value of a feature.

776 Unlike Brown et al. (2020), we have not included derived petrophysical logs  
777 in this study. From a machine learning perspective, petrophysical logs such as  
778 water saturation, porosity and clay volume can be viewed as engineered features  
779 which augment or extend our view of the raw input data. Their addition to the  
780 imputation workflow may improve correlations and relationships between the  
781 raw data that were ignored previously. Future tests may consider using these  
782 data as input if available. Similar to the work of Brown et al. (2020), this would  
783 also result in imputed petrophysical products.

784 There are many ML algorithms and we have tested some of the easiest to  
785 implement. Deep learning such as convolutional neural networks which can  
786 better account for adjacency in samples may benefit from the MICE approach to  
787 imputation. Indeed, most ML methods cannot handle missing data so iterative  
788 imputation may improve these models.

## 789 **6. Conclusion**

790 Many subsurface analysis tasks and workflows rely upon or can benefit from a  
791 complete well logging data set. However, in many cases the logging measurements  
792 are rarely complete with gaps or logs missing entirely. This study has utilised  
793 the MICE approach to successfully and completely impute multiple well logs  
794 simultaneous using ML algorithms. Of the four algorithms that were tested,  
795 gradient boosted trees performed the best. Although MICE did not always  
796 improve the directed imputation of logs when using GBT, imputation when  
797 certain combinations of missing logs are missing may benefit from the iterative  
798 approach. MICE can also improve GBT results when the sparsity of the input  
799 data is high.

800 Finally, while GBT have the ability to naturally handle missing values in the  
801 input features, many ML algorithms cannot. MICE may prove more useful in  
802 scenarios where algorithms require complete input features for training.

### 803 **Computer code and data availability**

804 Source code used for analysis and log imputation using MICE is available from  
805 the first author and can be downloaded from [https://github.com/trhallam/  
806 mice\\_well\\_log\\_imputation](https://github.com/trhallam/mice_well_log_imputation).

807 The Volve well log data is available for download from the Volve Data  
808 Village provided by Equinor at [https://www.equinor.com/en/what-we-do/  
809 digitalisation-in-our-dna/volve-field-data-village-download.html](https://www.equinor.com/en/what-we-do/digitalisation-in-our-dna/volve-field-data-village-download.html).

810 The Force 2020 data is available for download from Xeek [https://xeek.ai/  
811 challenges/force-well-logs/overview](https://xeek.ai/challenges/force-well-logs/overview).

### 812 **Declaration of competing interest**

813 The authors declare that they have no known competing financial interests or  
814 personal relationships that could have appeared to influence the work reported  
815 in this paper.

### 816 **Authorship statement**

817 Antony Hallam developed the methodology, the code, worked on the applica-  
818 tion and the writing; Debajoy Mukherjee developed the code and methodology;  
819 Romain Chassagne discussed the methodology, supervised the research and  
820 writing.

### 821 *Acknowledgements*

822 We would like to thank the sponsors of the Edinburgh Time-Lapse Project,  
823 Phase VII: AkerBP, BP, CGG, Chevron/Ithaca Energy CNOOC, Equinor, Cono-  
824 coPhillips, ENI, Petrobras, Norsar, Woodside, Taqa, Halliburton, ExxonMobil,  
825 OMV and Shell for financial support. Equinor for provision of the Volve public  
826 dataset. The FORCE 2020 sponsors and the Norwegian Government for the

827 F2020 dataset. Thank you to colleagues and peers for their help and feedback.  
828 We also acknowledge Schlumberger for the use of their software and the Python  
829 open source community.

## 830 References

- 831 Azur, M. J., Stuart, E. A., Grangakis, C., and Leaf, P. J. (2011). Multiple impu-  
832 tation by chained equations: what is it and how does it work? *International*  
833 *Journal of Methods in Psychiatric Research*, 20(1):40–49.
- 834 Bormann, P., Aursand, P., Dilib, F., and Dischington, P d Manral, S. (2020).  
835 2020 FORCE Machine Learning Contest.
- 836 Brown, N., Roubíčková, A., Lampaki, I., MacGregor, L., Ellis, M., and Vera  
837 de Newton, P. (2020). Machine learning on Crays to optimize petrophysical  
838 workflows in oil and gas exploration. *Concurrency Computation*, 32(20).
- 839 Bukar, I., Adamu, M. B., and Hassan, U. (2019). A machine learning approach  
840 to shear sonic log prediction. *Society of Petroleum Engineers - SPE Nigeria*  
841 *Annual International Conference and Exhibition 2019, NAIC 2019*.
- 842 Christ, M., Braun, N., Neuffer, J., and Kempa-Liehr, A. W. (2018). Time series  
843 feature extraction on basis of scalable hypothesis tests (tsfresh – a python  
844 package). *Neurocomputing*, 307:72 – 77.
- 845 Churikov, S. N. and Grafeeva, N. (2018). Recovering gaps in the gamma-ray  
846 logging method. *International Multidisciplinary Scientific GeoConference*  
847 *Surveying Geology and Mining Ecology Management, SGEM*, 18(2.2):361–368.
- 848 Diaz, J. L. G. and Zadrozny, B. (2020). Propagation of Well-Log Data Imputation  
849 Uncertainties Towards the Interpolated 3D-Petrophysical Map Using Epistemic  
850 Kernels and Kriging. In *EAGE 82nd Conference and Exhibition*, number  
851 December 2020, Amsterdam, Netherlands. EAGE.

- 852 Dramsch, J. S. (2020). Chapter one - 70 years of machine learning in geoscience  
853 in review. In Moseley, B. and Krischer, L., editors, *Machine Learning in*  
854 *Geosciences*, volume 61 of *Advances in Geophysics*, pages 1–55. Elsevier.
- 855 Dubey, H. and Pudi, V. (2013). Cluekr : Clustering based efficient knn regression.  
856 In Pei, J., Tseng, V. S., Cao, L., Motoda, H., and Xu, G., editors, *Advances*  
857 *in Knowledge Discovery and Data Mining*, pages 450–458, Berlin, Heidelberg.  
858 Springer Berlin Heidelberg.
- 859 Feng, R., Grana, D., and Balling, N. (2021). Imputation of missing well log  
860 data by random forest and its uncertainty analysis. *Computers & Geosciences*,  
861 152(March):104763.
- 862 Freund, Y. and Schapire, R. E. (1997). A Decision-Theoretic Generalization of  
863 On-Line Learning and an Application to Boosting. *Journal of Computer and*  
864 *System Sciences*, 55(1):119–139.
- 865 Gardner, G. H. F., Gardner, L. W., and Gregory, A. R. (1974). Formation  
866 Velocity and Density - The diagnostic for stratigraphic traps. *Geophysics*,  
867 39(6):770–780.
- 868 Ghaithi, A. A. (2020). *Deep Learning Methods for Shear Log Predictions in the*  
869 *Volve Field Norwegian North Sea*. Master of science (geophysical engineering),  
870 Colorado School of Mines.
- 871 Greenberg, M. L. and Castagna, J. P. (1992). Shear-wave velocity estimation in  
872 porous rocks: theoretical formulation, preliminary verification and applications.  
873 *Geophysical Prospecting*, 40(2):195–209.
- 874 Hallam, T., MacBeth, C., Chassagne, R., and Amini, H. (2020). 4D seismic study  
875 of the Volve Field - an open subsurface-dataset. *First Break*, 38(2):59–70.
- 876 Hampson, D. P., Schuelke, J. S., and Quirein, J. A. (2001). Use of multiattribute  
877 transforms to predict log properties from seismic data. *Geophysics*, 66(1):220–  
878 236.

- 879 Hegde, C. and Gray, K. E. (2017). Use of machine learning and data analytics  
880 to increase drilling efficiency for nearby wells. *Journal of Natural Gas Science*  
881 *and Engineering*, 40:327–335.
- 882 James, G., Witten, D., Hastie, T., and Tibshirani, R. (2013). *An Introduction*  
883 *to Statistical Learning with Applications in R*. Springer-Verlag, New York, 7  
884 edition.
- 885 Jian, H., Chenghui, L., Zhimin, C., and Haiwei, M. (2020). Integration of  
886 deep neural networks and ensemble learning machines for missing well logs  
887 estimation. *Flow Measurement and Instrumentation*, 73:101748.
- 888 Ke, G., Meng, Q., Finley, T., Wang, T., Chen, W., Ma, W., Ye, Q., and Liu, T. Y.  
889 (2017). LightGBM: A highly efficient gradient boosting decision tree. *Advances*  
890 *in Neural Information Processing Systems*, 2017-December(Nips):3147–3155.
- 891 Lopes, R. L. and Jorge, A. M. (2018). Assessment of predictive learning methods  
892 for the completion of gaps in well log data. *Journal of Petroleum Science and*  
893 *Engineering*, 162(November):873–886.
- 894 Lundberg, S. M., Erion, G., Chen, H., DeGrave, A., Prutkin, J. M., Nair, B.,  
895 Katz, R., Himmelfarb, J., Bansal, N., and Lee, S.-I. (2020). From local  
896 explanations to global understanding with explainable AI for trees. *Nature*  
897 *Machine Intelligence*, 2(1):56–67.
- 898 Lundberg, S. M. and Lee, S.-I. (2017). A unified approach to interpreting model  
899 predictions. In Guyon, I., Luxburg, U. V., Bengio, S., Wallach, H., Fergus, R.,  
900 Vishwanathan, S., and Garnett, R., editors, *Advances in Neural Information*  
901 *Processing Systems 30*, pages 4765–4774. Curran Associates, Inc.
- 902 Murray, J. S. (2018). Multiple imputation: A review of practical and theoretical  
903 findings. *Statistical Science*, 33(2):142–159.
- 904 Poloczek, J., Treiber, N. A., and Kramer, O. (2014). Knn regression as geo-  
905 imputation method for spatio-temporal wind data. In de la Puerta, J. G.,

- 906 Ferreira, I. G., Bringas, P. G., Klett, F., Abraham, A., de Carvalho, A. C.,  
907 Herrero, Á., Baruque, B., Quintián, H., and Corchado, E., editors, *Inter-*  
908 *national Joint Conference SOCO'14-CISIS'14-ICEUTE'14*, pages 185–193,  
909 Cham. Springer International Publishing.
- 910 Raghunathan, T. E., Lepkowski, J. M., Hoewyk, J. V., and Solenberger, P.  
911 (2001). A Multivariate Technique for Multiply Imputing Missing Values Using  
912 a Sequence of Regression Models. *Survey Methodology*, 27(1):85–95.
- 913 Russell, B. H., Hampson, D. P., and Lines, L. R. (2003). Application of the  
914 radial basis function neural network to the prediction of log properties from  
915 seismic attributes - A channel sand case study. *2003 SEG Annual Meeting*,  
916 pages 1–4.
- 917 Sarkar, D., Bali, R., and Sharma, T. (2018). *Practical Machine Learning with*  
918 *Python*. Springer Science, New York.
- 919 Tipping, M. E. (2001). Sparse Bayesian Learning and the Relevance Vector  
920 Machine. *Journal of Machine Learning Research*, 1(3):211–244.
- 921 Tittman, J. (1986). Geophysical well logging. page 186.
- 922 van Buuren, S. (2007). Multiple imputation of discrete and continuous data  
923 by fully conditional specification. *Statistical Methods in Medical Research*,  
924 16(3):219–242.
- 925 van Buuren, S. and Groothuis-Oudshoorn, K. (2011). mice: Multivariate impu-  
926 tation by chained equations in R. *Journal of Statistical Software*, 45(3):1–67.
- 927 Varoquaux, G., Buitinck, L., Louppe, G., Grisel, O., Pedregosa, F., and Mueller,  
928 A. (2015). Scikit-learn. *GetMobile: Mobile Computing and Communications*,  
929 19(1):29–33.

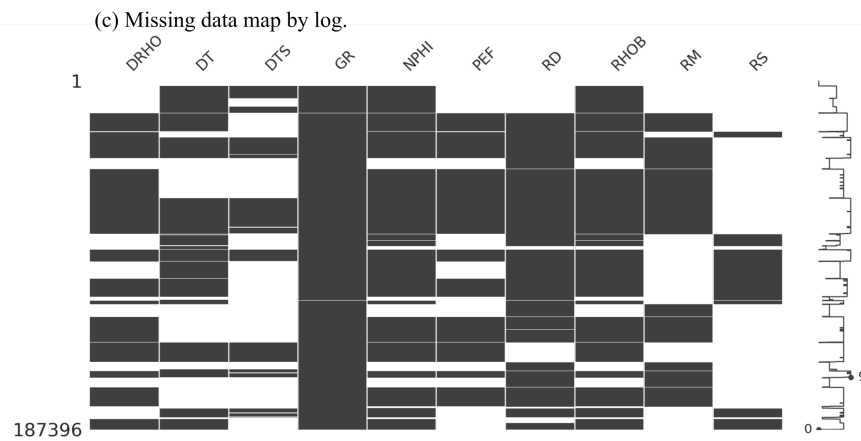
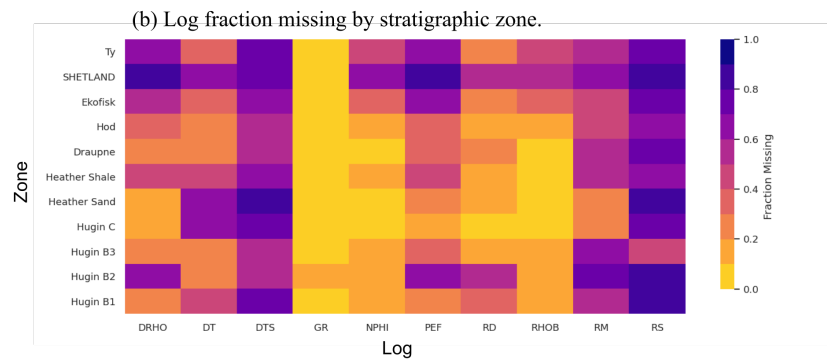
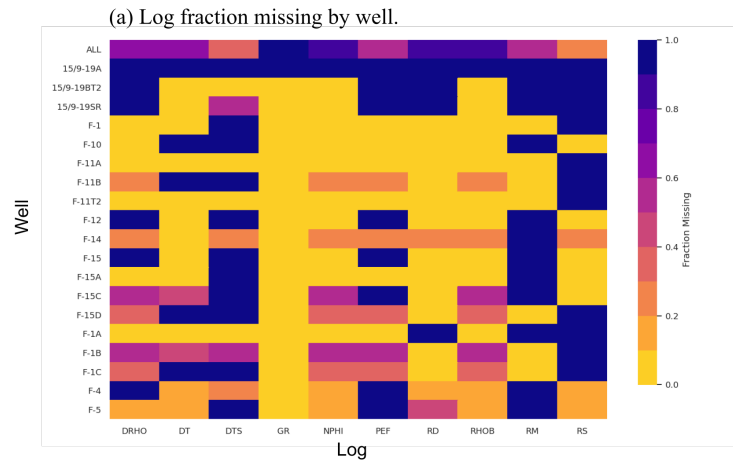


Figure 1: Missing data characterisation for Volve data set. (c) white is for missing data



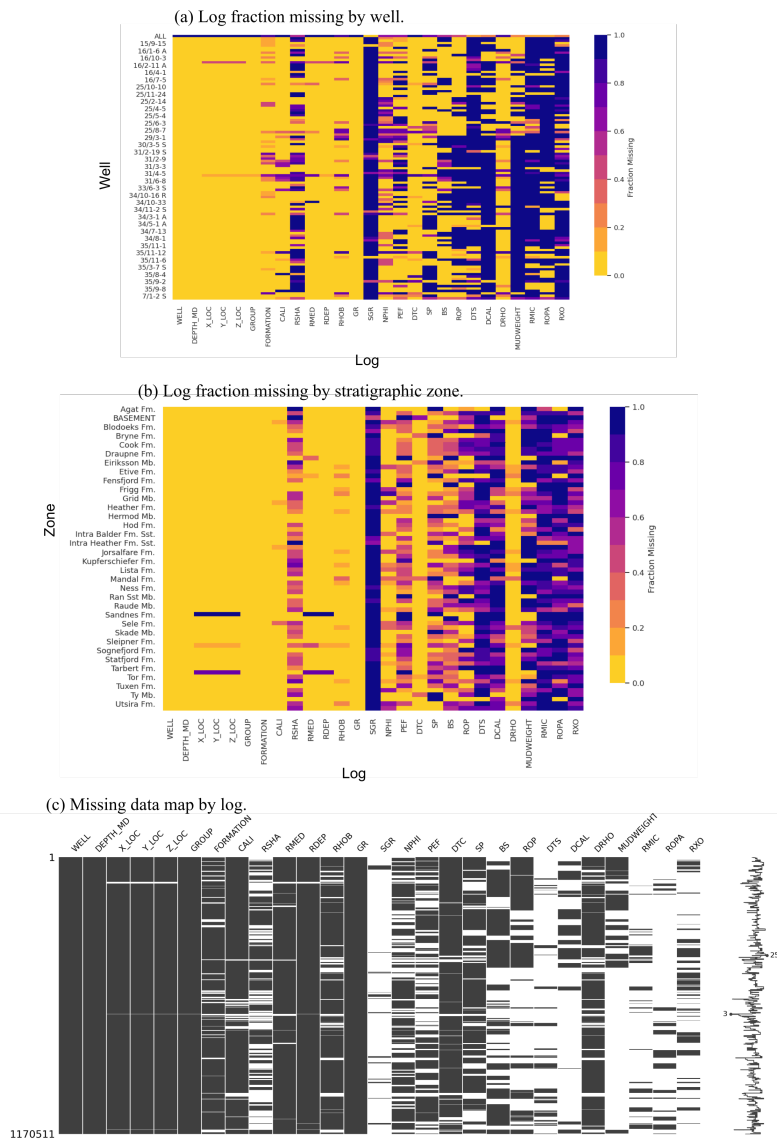


Figure 2: Missing data characterisation for Force 2020 and Volve data set.

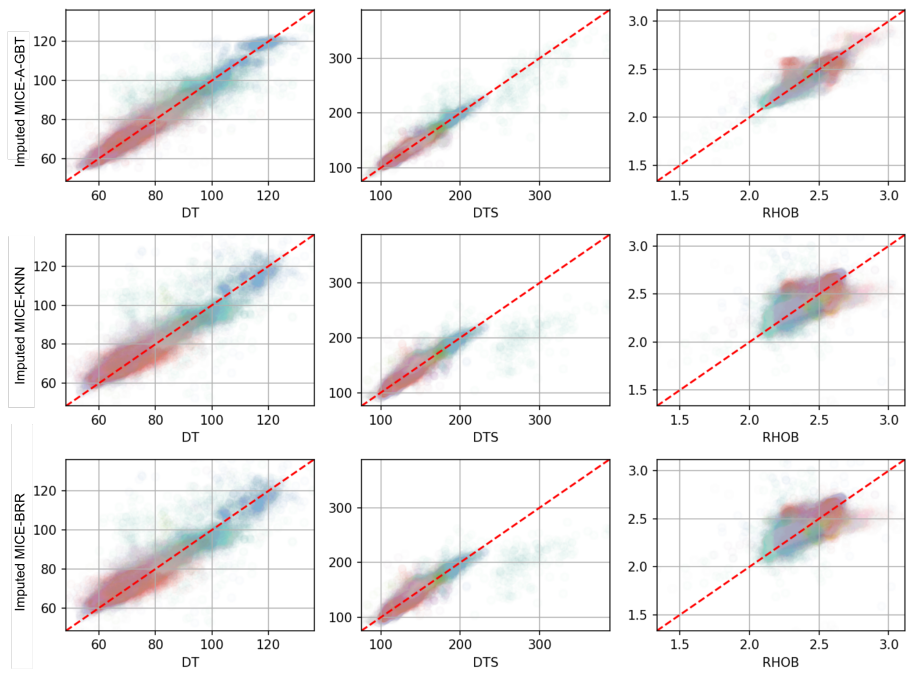


Figure 3: Recorded versus Imputed Results for DT, DTS and RHOB logs using MICE-A-GBT (top) MICE-KNN (middle) and MICE-BRR (bottom). Points are coloured by stratigraphic zone. Intensity of colour corresponds to the density of samples.

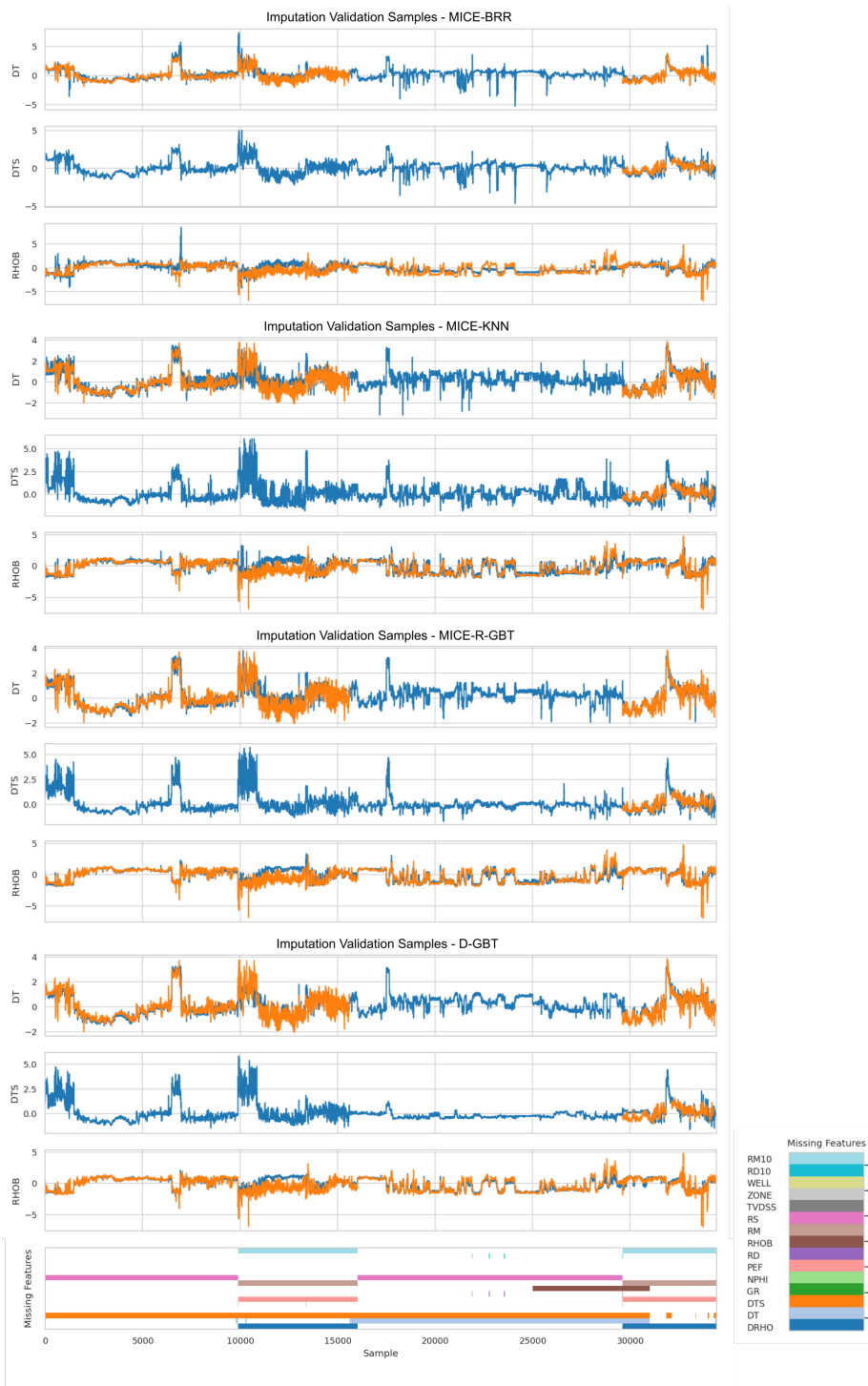


Figure 4: Test data imputation and prediction with the four tested imputation models. Imputed values are in blue and true values in orange. The bottom frame shows missing values of the input features prior to imputation.

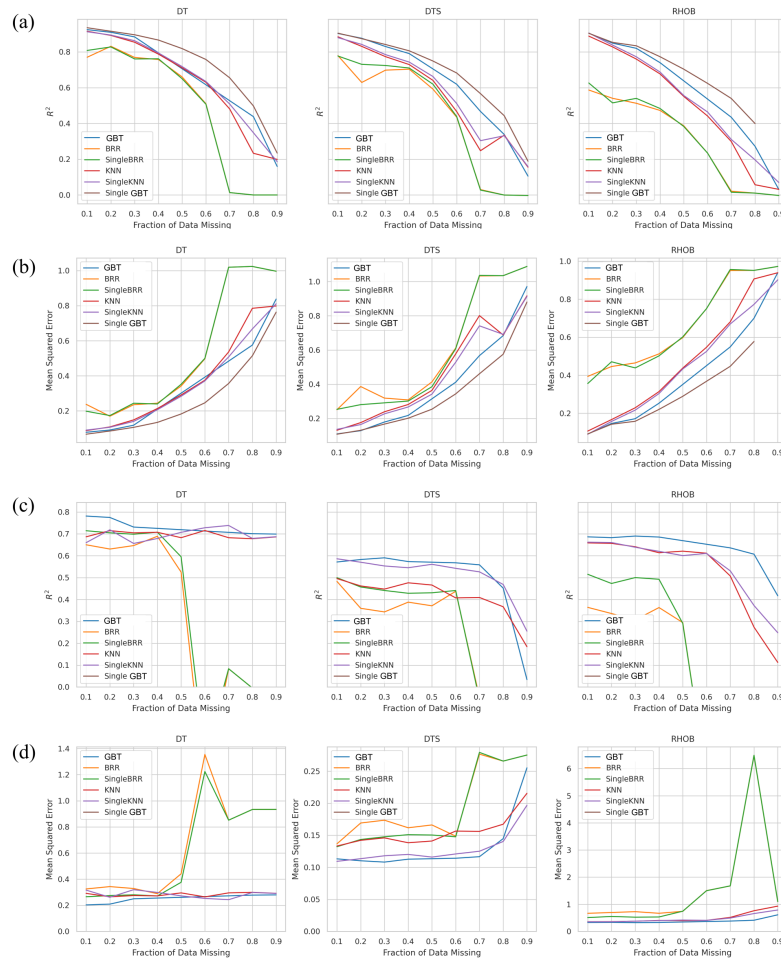


Figure 5: Volve test results for increasing sparsity of input data; (a, b)  $R^2$  and MSE for validation data, (c, d)  $R^2$  and MSE for test data.

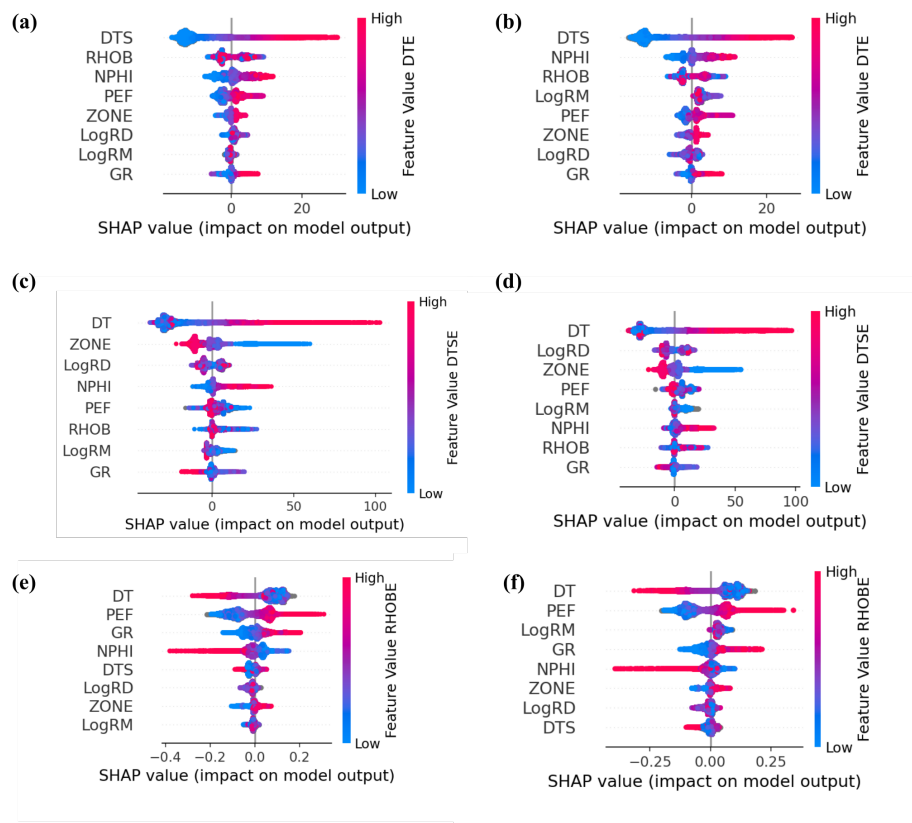


Figure 6: SHAP Values for second and last imputation rounds of MICE-A-GBT models for (a, b) DT, (c, d) DTS, and (e, f) RHOB.

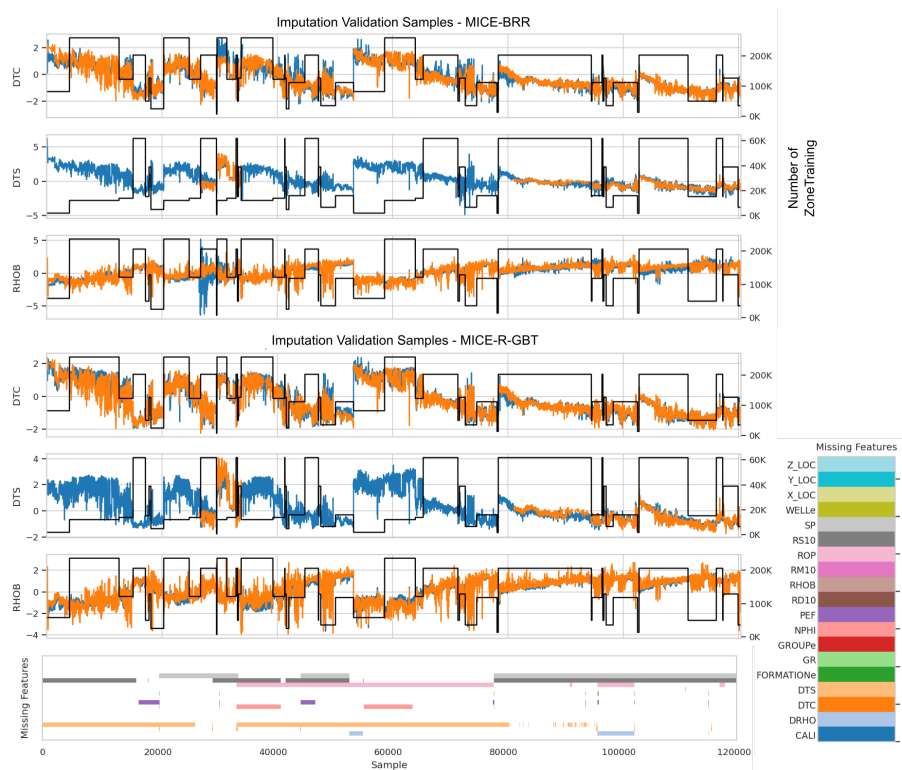


Figure 7: Force 2020 test data imputation and prediction with the MICE-BRR and MICE-R-GBT model. Imputed values are in blue and true values in orange. The bottom frame shows missing values of the input features prior to imputation and the black line (right axis) indicates the number of samples available for training in that geological super group.

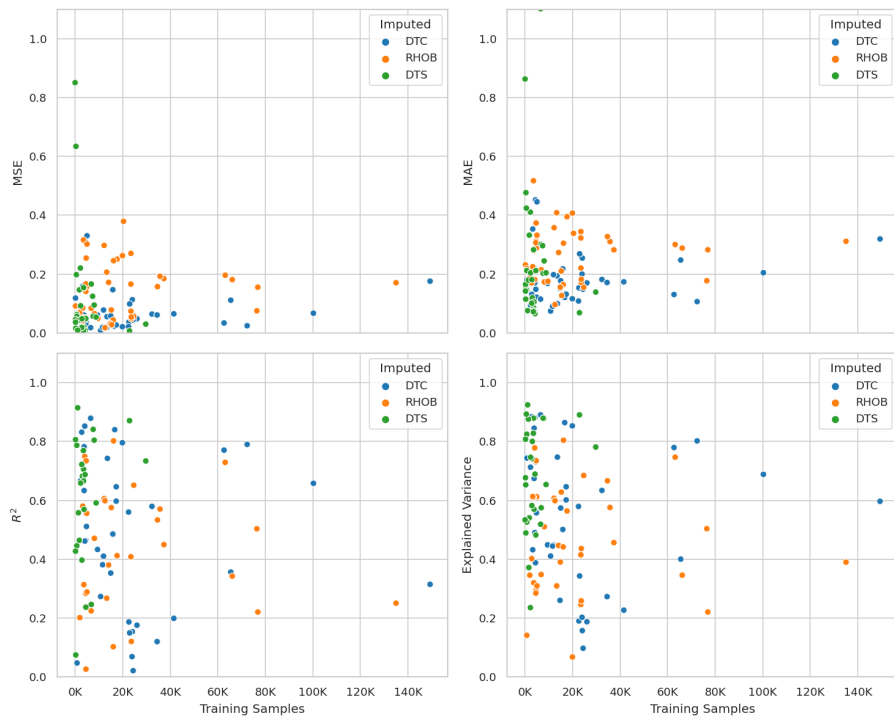


Figure 8: Force 2020 error metrics plotted by imputed target and geological formation for the MICE-A-GBT model.